ELSEVIER

Biochimica et Biophysica Acta 1295 (1996) 34–43

BBA Biochimica et Biophysica Acta

Purification and sequencing of multiple forms of *Brassica napus* seed napin large chains that are calmodulin antagonists and substrates for plant calcium-dependent protein kinase

Gregory M. Neumann [a], Rosemary Condron [a], Ian Thomas [b], Gideon M. Polya [a,*]

[a] *School of Biochemistry, La Trobe University, Bundoora, Victoria 3083, Australia*
[b] *School of Chemistry, La Trobe University, Bundoora, Victoria 3083, Australia*

Received 15 December 1995; accepted 11 January 1996

Abstract

Six napin large (L) chains (as well as six napin small chains) were resolved from the seeds of kohlrabi (*Brassica napus* var. rapifera) by a procedure involving extraction, batchwise elution from carboxymethylcellulose (CM52) and reversed-phase HPLC after treatment with guanidine hydrochloride and 2-mercaptoethanol. The precise average molecular masses of the circa 4.5 kDa small subunits and the circa 10 kDa large subunits were determined by electrospray ionisation mass spectrometry (ESMS). Of six large subunits resolved (L1A, L1B, L1C, L2A, L2B and L2C), the complete amino acid sequences of four (L1A, L2A, L2B and L2C) and the near-complete sequences of two (L1B and L1C) were deduced from the ESMS-based masses of tryptic fragments, Edman sequencing and previously published data. The deduced structures are precisely consistent with this data and with the ESMS-based average molecular masses of these polypeptides. ESMS analysis of unreduced napin extract revealed only seven circa 14.5 kDa complexes, the observed masses being in close agreement with those calculated for 1:1 complexes of particular small and large subunits assuming four disulfides in each napin complex. The structures of the napin large subunits (86–91 residues) are very similar and all amino acid differences observed are confined to only 25 positions. The L2A, L2B and L2C large chains (but not the L1A, L1B and L1C large chains) are phosphorylated well by plant Ca^{2+}-dependent protein kinase (CDPK). The CDPK-catalyzed phosphorylation site on the large chain L2A is inferred to be S^{57} within the sequence LQQVIS^{57}RIYQT (the site being S^{60} within the same sequence in L2B and L2C). The napin-containing basic protein fraction from *B. napus* seeds largely abolishes the Ca^{2+}-dependent fluorescence enhancement of dansyl-calmodulin and also inhibits calmodulin (CaM)-dependent myosin light chain kinase (MLCK). The resolved napin long chains also inhibit MLCK. Each kohlrabi large chain contains 2 sequences (corresponding to L^{10}-Q^{20} and Q^{51}-L^{64} of L1A) which have the potential to form amphipathic α-helices. Each large chain also contains a Q-rich 19 amino acid sequence (corresponding to L^{30}-Q^{48} of L1A) which has the potential to form a '2-sided' α-helix with basic residues confined to one side. These structural elements may be involved in the inferred interaction of these proteins with CaM and may be relevant to the biological activity of antifungal proteins of this kind.

Keywords: Calmodulin antagonist; Calmodulin substrate; Calcium-dependent protein kinase; (*B. napus*)

1. Introduction

Napins are storage proteins with antifungal properties that are elaborated by plants, notably those of the Brassicaceae [1–16]. The napins are composed of 1:1 disulfide-linked complexes of circa 4.5 kDa small and circa 10 kDa large chains [6,8,9]. The small chains are composed of about 40 amino acids including 2 cysteine residues. The large chains are composed of about 90 amino acids including 6 cysteine residues [1–16]. The 1:1 complexes involve two interchain disulfide linkages [6,8,9]. These abundant seed proteins appear to have a number of functions. They are nitrogen-rich 'storage proteins' and disappear during seed germination [17]. The 14.5 kDa complexes are protease inhibitors [9,16]. The napins are potent antifungal proteins [4,14] and can also act synergistically with α- and β-thionins in this respect [14]. The napin complexes and the isolated small subunits are also calmodulin (CaM) antagonists [15,18] and the CaM antagonist activity of

Abbreviations: CDPK, Ca^{2+}-dependent protein kinase; DTT, dithiothreitol; EGTA, ethylene glycol bis(β-aminoethyl ether)-*N,N,N',N'*-tetraacetic acid; ESMS, electrospray ionization mass spectrometry; TFA, trifluoroacetic acid; TPCK, L-(1-tosylamido-2-phenyl)ethylchloromethyl ketone.

* Corresponding author. Fax: +61 3 94792467.

PII S0167-4838(96)00007-6

radish seeds disappears, together with the napins, during seed germination [17]. Napin small chains [15,18] and large chains [18] can be phosphorylated by plant Ca^{2+}-dependent protein kinase (CDPK). However a biological function for this is not known.

There can be a multiplicity of napins encoded by particular plant genomes. Thus, for example, kohlrabi seeds contain at least six different small chains and six different large chains [18], radish seeds contain at least four small chain variants [15] and four napin genes have been resolved from *Arabidopsis thaliana* [3]. The small chain sequences involve short N-terminal P-, A/G- and S-containing sequences bounding Q-rich circa 24 amino acid central sequences [15,18]. Amphipathic α-helix wheel projection analysis shows that the Brassicaceae napin small chain central domains have the potential to form '2-sided' α-helices in which all the basic residues are located on one side of each helix [15,18]. This structure may be involved in the CaM antagonist and other bioactivities of these antifungal protein subunits [15,18]. The present paper describes the determination of the primary structures of six napin large chains from kohlrabi through comparison of data from electrospray ionization mass spectrometry (ESMS) and limited N-terminal Edman sequencing with published napin sequences. This paper also reports that napin large chains are CaM antagonists (as are the small chains) and can be phosphorylated at a particular site by signal-regulated plant CDPK.

2. Materials and methods

2.1. Purification of kohlrabi seed napin large chains

Kohlrabi (*Brassica napus* var. rapifera) seeds (100 g) were extracted and the napin-containing fraction isolated as described in the accompanying paper [18]. In brief, this procedure successively involved freezing seeds in liquid N_2, grinding to a powder, repeated extraction in water, removal by centrifugation of proteins precipitated by acid treatment (pH 5.0) and heating (70°C/5 min), batchwise elution from carboxymethylcellulose (CM52) and gel filtration on a Sephadex G-50 column in 50 mM ammonium acetate (pH 5.0). This final procedure yields two well-resolved broad peaks of protein, the peak eluting at higher elution volume containing CDPK substrate activity and napins [18].

The napin large chains were separated from the small subunits by a procedure successively involving prior phosphorylation using [γ-^{32}P]ATP and wheat embryo CDPK, treatment with 3 M guanidine-HCl and 2-mercaptoethanol, elution from a C18 Sep-Pak in 50% CH_3CN in 0.1% TFA and finally reversed-phase HPLC on a C18 column (Vydac; 4.6 mm × 25 cm; 5 μm particle size) fitted with a C8 guard column (Aquapore RP300; 4.6 mm × 30 mm; 7 μm particle size). The column was eluted with a linear gradient of increasing CH_3CN in 0.1% TFA (flow rate 1 ml/min; 0–50% CH_3CN in 50 min) [18]. ^{32}P in the HPLC fractions was measured by Cerenkov counting and compared with the UV absorbance at 220 nm to identify the major peaks of CDPK protein substrate. This procedure resolved 4 small subunit fractions (S1, S2, S3 and S4, eluting at 33, 35, 38 and 39% CH_3CN concentration, respectively) and 2 large subunit fractions (L1 and L2, eluting at 44% and 46% CH_3CN concentration, respectively) [18]. To remove CH_3CN and TFA, HPLC fractions were concentrated to dryness in a SpeedVac vacuum concentrator followed by solubilization in 80 μl distilled water. Concentrated fractions were then assayed for MLCK inhibitory activity and analysed by electrospray ionization mass spectrometry (ESMS).

2.2. Tryptic digestion, phosphorylation site determination and phosphoamino acid analysis

^{32}P-Labeled phosphorylated L1 and L2 fraction proteins from C_{18} reversed-phase HPLC were subjected to tryptic digestion (10–100 μg protein, 0.5–5 μg trypsin in 100 mM NH_4HCO_3, 4 mM DTT, 1 mM $CaCl_2$ for 20 h at room temperature) followed by acidification with 0.1% TFA and C_{18} reversed-phase HPLC. CDPK phosphorylation sites were inferred from the locations of ^{32}P-labeled phosphopeptides identified by Cerenkov counting of HPLC fractions. Peptides were characterised by ESMS and N-terminal Edman sequencing where necessary. High voltage electrophoresis was used to conduct phosphoamino acid analyses of ^{32}P-labeled phosphoproteins hydrolysed in 6 M HCl for 1 h at 110°C. Electrophoresis was carried out for 3–4 h at 4 kV and pH 2.6 in a running buffer containing 0.2% (v/v) pyridine and 10% (v/v) glacial acetic acid, followed by ninhydrin detection of internal standards (600 nmol each of phospho-L-tyrosine, phospho-L-threonine and phospho-L-serine). ^{32}P was measured along the migration axis by Cerenkov counting of 1 cm wide strips of the electrophoresis paper (Whatman 3MM).

2.3. Protein phosphorylation and dansyl-calmodulin fluorescence

Wheat embryo CDPK [19] and CaM-dependent MLCK [19] were purified and assayed radiochemically as described previously [20]. Dansyl-calmodulin was synthesized through the reaction of dansylchloride with purified wheat germ calmodulin and Ca^{2+}-dependent fluorescence changes measured as described previously [30]. All materials for protein isolation and analysis of protein phosphorylation were as detailed in the accompanying paper [18].

2.4. Amino acid sequencing and electrospray ionisation mass spectrometry

Amino acid sequencing by sequential Edman degradation was conducted using an Applied Biosystems 470A gas

phase peptide sequenator coupled to an Applied Biosystems 130A separation system for automatic on-line analysis of PTH amino acids. ESMS of proteins and peptides was carried out on a VG BIO-Q electrospray mass spectrometer (VG Biotech, Cheshire, UK) using 5–500 pmol samples in 10 μl of 50% methanol (containing 1% acetic acid), a flow rate of 3 μl/min and data acquisition over several minutes, during which time the quadrupole mass spectrometer was typically scanned 10–30-times over the range m/z 300 to m/z 1400 at unit mass resolution. The mass scale was calibrated using multiply charged ions from the separate introduction of myoglobin.

3. Results

3.1. Resolution of kohlrabi seed napin large chains

B. napus seed napins were isolated as described in Section 2 by a procedure involving batchwise chromatography on carboxymethylcellulose (Whatman CM-52) followed by gel filtration. Gel filtration resolves 2 broad protein peaks. The material associated with the peak at higher elution volume serves as a substrate for wheat embryo Ca^{2+}-dependent protein kinase (CDPK) and consists mainly of napins, as subsequently demonstrated [18].

The CDPK substrate material resolved by gel filtration [18] was phosphorylated in a reaction employing wheat embryo CDPK and [γ-^{32}P]ATP. Treatment with 3 M guanidine-HCl and 2-mercaptoethanol, followed by reversed-phase HPLC on a C18 column eluted with a gradient of increasing CH_3CN concentration in 0.1% TFA, resolved four major small subunit fractions (S1, S2, S3 and S4, eluting at 33%, 35%, 38% and 39% CH_3CN in 0.1% TFA, respectively) and 2 large subunit fractions L1 and L2, eluting at 44% and 46% CH_3CN in 0.1% TFA, respectively) [18]. The 6 napin small chains present in fractions S1-S4 have been completely sequenced by Edman sequencing, and ESMS and comparison with published sequences [18]. Of the two fractions corresponding to napin large chains (L1 and L2), only the L2 fraction is phosphorylated substantially [18].

Table 1
Average molecular masses of *B. napus* large chains

Polypeptide	Relative intensity	Average molecular mass (Da)	
		observed	calculated
L1A	100%	9549.0 ± 1.6	9548.12
L1B	50%	9824.7 ± 2.0	9824.35
L1C	20%	9853.1 ± 2.2	9852.37
L2A	100%	9815.1 ± 1.1	9815.36
L2B	80%	10275.6 ± 1.1	10275.81
L2C	40%	10186.9 ± 1.2	10186.72

The observed average molecular masses and relative intensities were determined by electrospray ionization mass spectrometry (ESMS). 95% confidence limits are given. The calculated average molecular masses were determined from the deduced amino acid sequences (Fig. 5) assuming all cysteine residues to be in the reduced form.

ESMS applied to the L1 and L2 fractions revealed components L1A (9549.0 ± 1.6 Da), L1B (9824.7 ± 2.0 Da) and L1C (9853.1 ± 2.2 Da) from fraction L1 and L2A (9815.1 ± 1.1 Da), L2B (10275.6 ± 1.1 Da), and L2C (10186.9 ± 1.2 Da) from fraction L2 (Table 1).

3.2. Complete sequences of kohlrabi napin large chains

The phosphorylated napin large chain fractions L1 and L2 were digested with trypsin and the digest fractionated by reversed-phase HPLC on a C18 column (Figs. 1 and 2).

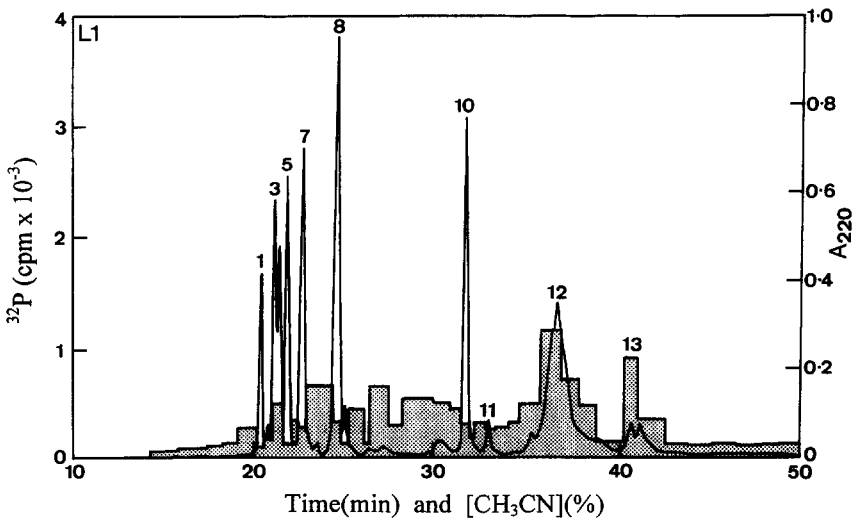

Fig. 1. Reversed-phase HPLC of a tryptic digest of ^{32}P-labeled phosphorylated fraction L1 napin large chains. Fraction L1 was phosphorylated using [γ-^{32}P]ATP and CDPK and the subsequently generated tryptic digest fragments resolved by reversed-phase HPLC on a C_{18} column eluted with a gradient of increasing CH_3CN concentration in 0.1% TFA as described in Section 2. Histogram height, ^{32}P cpm; continuous trace, A_{220}.

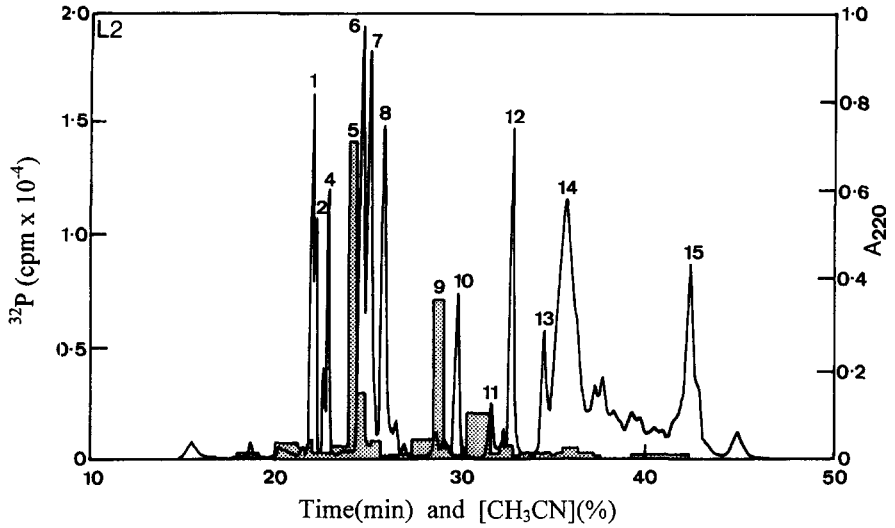

Fig. 2. Reversed-phase HPLC of a tryptic digest of ^{32}P-labeled phosphorylated fraction L2 napin large chains. Other details are as for the legend to Fig. 1.

The tryptic fragments were analysed by ESMS (Figs. 3 and 4) and selected fragments subjected to N-terminal Edman sequencing (Table 2). By comparison with previously published kohlrabi napin large chain sequence data [9] it was possible to identify and assign the observed tryptic fragments on the basis of their ESMS-derived masses coupled with Edman sequencing where necessary.

The complete sequence of L1A was deduced in this manner from the sequences of sequential tryptic fragments deduced from previously published *B. napus* napin large chain sequence data [6,7,9,12] coupled with Edman sequencing (Table 2) and precise agreement of calculated masses and observed ESMS-derived masses of tryptic fragments (Fig. 3). The deduced sequence of L1A (Fig. 5) is in exact agreement with this data. The only fragments not found were those comprising GASKAVK[38], a sequence which is highly conserved in *Brassica* napins (Fig. 5). If this sequence is assumed to be present in L1A, close agreement is obtained between the observed L1A ESMS mass (9549.0 ± 1.6 Da; Table 1) and that calculated from the deduced sequence (9548.12 Da; Fig. 5). The sequence of residues 39–50 of L1A, Q[39]QIQQQGQQQGK, which occurs within a variable region [9], was inferred from the same sort of evidence and confirmed directly by Edman sequencing (Table 2).

The sequence deduced for L1A is identical to that of the cDNA-based sequence of a *B. napus* napin large chain [1,2,6] (sequence 1, Fig. 5) except for the absence of a C-terminal Y in L1A (Fig. 5).

ESMS analysis of fraction L1 gave evidence of an additional major component L1B and a minor component L1C with masses of 9824.7 ± 2.0 Da and 9853.1 ± 2.2 Da, respectively (Table 1). The presence of additional large chain components in fraction L1 was confirmed by the

Tryptic fragment peak	Peak elution [CH_3CN] (%)		Sequence assignment	Average molecular mass (Da)	
				Observed	Calculated
L1(12)a	36.6	L1A(1-31)	PQGPQQRPPLLQQCCNELHQEEPLCVCPTLK (ox)	3524.9 ± 1.4	3524.09
L1(12)b	36.6	L1B/C(1-31) [L1A/B(32-38)	SQGPQQRPPLLQQCCNELHQEEPLCVCPTLK (ox) GASKAVK]	3513.6 ± 1.2	3514.05
L1(1)	20.4	L1A(39-50) [L1B/C(39-40)	QQIQQQGQQQGK SR]	1398.4 ± 0.7	1398.50
L1(7)b	22.8	L1B/C(41-58)	TQPQGQMQGQQQQQIVSR	2069.1 ± 2.2	2070.28
L1(4)	21.4	L1A(51-56)	QQMVSR	747.7 ± 0.4	747.89
L1(8)	24.7	L1A(57-66)	IYQTATHLPK	1171.0 ± 0.6	1171.36
L1(3)	21.2	L1B/C(59-64)	IYQTAK	722.6 ± 0.4	722.84
L1(6)	22.0	L1B(65-68)	HLPR	521.6 ± 0.5	521.62
L1(10)	31.7	L1A(67-80), L1B/C(69-82)	VCNIPQVSVCPFQK (ox)	1559.6 ± 0.5	1559.87
L1(5)	21.9	L1A(81-86)	TMPGPS	588.5 ± 0.5	588.69
L1(7)a	22.8	L1B/C(83-88)	TTPGPY	634.4 ± 0.7	634.74

Fig. 3. Average molecular masses of sequential tryptic fragments of *B. napus* large subunits L1A, L1B and L1C. The fragments from a tryptic digest of ^{32}P-labeled phosphorylated fraction L1 (containing L1A, L1B and L1C) were resolved by reversed-phase HPLC (Fig. 1). Average molecular masses were determined by ESMS. 95% confidence limits are given. All of the calculated masses were determined assuming cysteine residues to be in the reduced form except where the oxidized form (ox) is indicated. Fragments contained in a single peak fraction and resolved by ESMS are indicated by a, b, in order of relative intensity. Fragments in square brackets were not observed (see text).

Tryptic fragment peak	Peak elution [CH_3CN] (%)	Sequence assignment		Average molecular mass (Da)	
				Observed	Calculated
L2(14)a	35.5	L2A/B(1-31)	PQSPQQRPPLLQQCCNELHQEEPLCVCPTLK (ox)	3554.1 ± 1.2	3554.12
L2(14)b	35.5	L2C(1-31)	PQGPQQRPPLLQQCCNELHQEEPLCVCPTLK (ox)	3524.5 ± 1.4	3524.09
L2(15)a	42.3	L2A/B(1-31)	PQSPQQRPPLLQQCCNELHQEEPLCVCPTLK (red)	3557.6 ± 1.3	3558.15
L2(15)b	42.3	L2C(1-31) [L2A/B/C(32-42)	PQGPQQRPPLLQQCCNELHQEEPLCVCPTLK (red) GASKAVKQQVR]	3527.4 ± 1.5	3528.12
L2(8)a	25.6	L2A(43-58)	QQQGQQQGQQLQQVISR	1854.0 ± 0.7	1854.06
L2(8)b	25.6	L2B/C(43-61)	QQGQQQGQQGQQLQQVISR	2167.4 ± 0.8	2167.37
L2(6)	24.3	L2A(59-68)	IYQTATHLPK	1171.3 ± 0.6	1171.36
L2(7)a	24.8	L2B/C(62-71)	IYQTATHLPR	1199.3 ± 0.6	1199.38
L2(11)	31.5	L2A(69-82)	VCNIPQVSVCPFQK (ox)	1559.2 ± 0.8	1559.88
L2(12)a	32.6	L2A(69-82)	VCNIPQVSVCPFQK (red)	1561.2 ± 0.8	1561.89
L2(7)b	24.8	L2A(69-88)	VCNIPQVSVCPFQKTMPGPS (ox)	2131.0 ± 0.8	2130.56
L2(12)b	32.6	L2C(72-85)	VCNIPQVSICPFQK (ox)	1573.3 ± 0.8	1573.90
L2(13)	34.3	L2C(72-85)	VCNIPQVSICPFQK (red)	1575.4 ± 0.8	1575.92
L2(3)	22.4	L2B(72-76)	VCNIR	603.4 ± 0.5	603.74
L2(10)	29.7	L2B(77-85)	QVSICPFQKQVSICPFQK	1048.8 ± 0.6	1049.26
L2(1)	21.7	L2A(83-88)	TMPGPS	588.3 ± 0.5	588.69
L2(4)	22.6	L2B/C(86-91)	TTPGPY	634.4 ± 0.5	634.70

Fig. 4. Average molecular masses of sequential tryptic fragments of *B. napus* napin large subunits L2A, L2B and L2C. Fragments from the tryptic digest of ^{32}P-labeled phosphorylated fraction L2 (containing L2A, L2B and L2C) were resolved by reversed-phase HPLC and analysed by ESMS. All other details are as for the legend to Fig. 3.

identification of tryptic fragments L1(12)b, L1(7)b, L1(3), L1(6) and L1(7)a (Fig. 3) which incorporate various single or multiple amino acid substitutions (Fig. 3) and include a variant C-terminal fragment TTPGPY^{88} (fragment L1(7)a; Fig. 3; Table 2). Only one further conservative change is required to account for the observed ESMS-derived mass of large chain L1B and that is the insertion of SR^{40} (Figs. 3 and 5) assuming minimal changes with respect to the other kohlrabi large subunit sequences found here. The deduced sequence yields a mass of 9824.35 Da (Fig. 5) consistent with the observed mass of 9824.7 ± 2.0 Da (Table 1). However it must be noted that while this deduced sequence is consistent with the observed fragments and fragment masses, the predicted tryptic frag-

```
                          1   5   10   15   20   25   30   35   40   45   50   55   60   65   70   75   80   85  90  93
                          .   .    .    .    .    .    .    .    .    .    .    .    .    .    .    .    .    .   .   .
L1A(9548.12 Da)           PQGPQQRPPLLQQCCNELHQEEPLCVCPTLKGASKAVKQQIQQQGQQQG-----KQQMVSRIYQTATHLPKVCNIPQVSVCPFQKTMPGPS --
L1B(9824.35 Da)           SQGPQQRPPLLQQCCNELHQEEPLCVCPTLKGASKAVKsrTQPQGQMQGQQ--Q-QQIVSRIYQTAKHLPRVCNIPQVSVCPFQKTTPGPY --
L1C(9852.37 Da)           SQGPQQRPPLLQQCCNELHQEEPLCVCPTLKGASKAVrsrTQPQGQMQGQQ--Q-QQIVSRIYQTAKHLPRVCNIPQVSVCPFQKTTPGPY --
L2A(9815.36 Da)           PQSPQQRPPLLQQCCNELHQEEPLCVCPTLKGASKAVKQQVRQQQ---GQQGQQLQQVISRIYQTATHLPKVCNIPQVSVCPFQKTMPGPS --
L2B(10275.81 Da)          PQSPQQRPPLLQQCCNELHQEEPLCVCPTLKGASKAVKQQVRQQGQQQGQQGQQLQQVISRIYQTATHLPRVCNIRQVSICPFQKTTPGPY --
L2C(10186.72 Da)          PQGPQQRPPLLQQCCNELHQEEPLCVCPTLKGASKAVKQQVRQQGQQQGQQGQQLQQVISRIYQTATHLPRVCNIPQVSICPFQKTTPGPY --

1.  pNAP1, napA
    pN2(9548.12 Da)       PQGPQQRPPLLQQCCNELHQEEPLCVCPTLKGASKAVKQQIQQQGQQQG-----KQQMVSRIYQTATHLPKVCNIPQVSVCPFQKTMPGPS(Y)-
2.  Ia(9459.03 Da)        PQGPQQRPPLLQQCCNELHQEEPLCVCPTLKGAAKAVKQQQQQQGQQQ------MQQVPSRIYQTATHLPKVCNIPQVSVCPFKKTMPGPS ---
3.  Ib(9560.18 Da)        PQGPQQRPPLLQQCCNELHQEEPLCVCPTLKGAAKAVKQQVRQQQQQQG------QQMVSRIYQTATHLPRVCNIRQVSICPFKKTMPGPG ---
4.  pN1(9781.24 Da)       QQGPQQRPPLHQQYCNELQQEEPLCVCPTLRGASKAVKQQIQQQEQQQG-----KQQMVNRIYQTATHLPKVCNIPQVSVCPFQKTMPGPS(Y)-
5.  BngNAP1(9785.36 Da)   PQGPQQRPPLLQQCCNELHQEEPLCVCPTLKGASKAVKQQVRQQQGQQGQQ---LQQVISRIYQTATHLPKVCNIPQVSVCPFQKTMPGPS(Y)-
6.  gNa(10146.73 Da)      QQGPQQRPPPPQQCCNELHQEEPLCVCPTLKGASKAVRQQVRQQQGQQM-QGQQMQQVISRVYQTATHLPRVCNIRQVSICPFQKTMPGPG(FY)
7.  napB(9547.22 Da)      PQGPQQRPPLLQQCCNELHQEEPLCVCPTLKGASKAVKQQIQQQGQQQG-----KLQMVSRIYQTATHLPKVCKIPQVSVCPFQKTMPGPS(Y)-
```

Fig. 5. Amino acid sequences of *B. napus* large chains. Complete deduced sequences of napin large chains L1A, L1B, L1C, L2A, L2B and L2C are aligned with each other. The numbering corresponds to the maximum number of alignable residue positions (95). All residues differing from the corresponding L1A amino acids are underlined. (-), space introduced for alignment. The reported sequences (1 to 7) of other *B. napus* napin large chains are also presented. Calculated average molecular masses are presented in parentheses. The references for the other *B. napus* napin large chains are as follows: 1, pNAP1 [6], napA [2], pN2 [1]; 2, Ia [9]; 3, Ib [9]; 4, pN1 [1]; 5, BngNAP1 [10]; 6, gNa [7]; 7, napB [12]. The C-terminal residues in parenthesis (Y and FY) indicate encoded residues in DNA-based sequences that may not be present in the processed product and the calculated masses for these sequences assuming that these residues are not present. The lower case letters (r,s) are hypothetical insertions in L1B and L1C that give average molecular masses in exact agreement with the observed masses but for which there is no other evidence.

Table 2
Edman sequencing of some tryptic fragments of *B. napus* large subunits

Fragment	Fragment N-terminal sequence
L1(1)	Q Q I Q Q Q G Q Q Q G K
L1(3)	I Y Q T A K
L1(4)	Q Q M V S R
L2(3)	V C N I R
L2(4)	T T P G P Y
L1(7)a	T T P G P Y
L1(7)b	T Q P Q G Q M Q G Q Q Q Q Q I V S R
L2(8)a	Q Q Q G Q Q G Q Q L Q Q V I S R
L2(8)b	Q Q G Q Q G Q Q G Q Q L Q Q V I S R

N-terminal sequences of selected tryptic fragments of napin large chains were determined by Edman degradation. The fragments are as defined in Figs. 1–4. Residues are underlined where assignment from Edman sequencing is equivocal or complicated by the presence of another sequence; however, all of these sequences have been confirmed from ESMS-based average molecular mass determinations (Figs. 3 and 4). C indicates a cysteine residue and S a serine residue based on the absence of a PTH-serine signal, the presence of a signal corresponding to the DTT adduct of PTH-dehydroalanine [21] and conservation of these residues in napin large chains (Fig. 5).

ments GASKAVK^{38} (or fragments thereof) (highly conserved in napin large chains) (Fig. 5) and SR^{40} were not actually resolved, possibly through loss in HPLC analysis.

The minor L1 fraction large chain L1C differs in mass from L1B by 28 Da (Table 1), which could be due to multiple substitutions or a single substitution such as in the sequence GASKAVRSR^{40}. There is precedence for this in that the *B. napus* gNa-encoded large chain has the sequence GASKAV*R*^{38} (sequence 6, Fig. 5) while all other napin large chains sequenced have the sequence GASKAVK^{38} (Fig. 5). Again it must be noted that fragments corresponding to GASK^{35}, AVR^{38} or SR^{40} were not actually observed. The calculated mass of this deduced sequence for L1C is 9852.37 Da (Fig. 5) in agreement with the observed mass (9853.1 ± 2.2 Da) (Table 1).

Fraction L2 contains three napin large chains L2A, L2B and L2C (Table 1). The complete sequence of napin L2A (Fig. 5) was similarly deduced from the available data (Tables 1 and 2; Figs. 4 and 5), the only L2A fragment (or parts thereof) not found in the tryptic digest of fraction L2 being the predicted fragment L2A (32–42) (GASKAVKQQVR^{42}). This missing sequence is consistent with other *B. napus* napin large chain sequences in this region (Fig. 5) and precisely accounts for the overall L2A mass when included in the deduced sequence (Fig. 5). The calculated overall mass of L2A is 9815.36 Da, as compared to the observed mass of 9815.1 ± 1.1 Da (Table 1). The remainder of the deduced L2A sequence is completely consistent with the observed tryptic fragment masses (Fig. 4) and Edman sequence information (Table 2).

The sequence deduced for L2B (Fig. 5) is consistent with Edman sequencing results and tryptic fragment masses. The mass of the deduced sequence (10275.81 Da) is in good agreement with the observed mass (10275.6 ± 1.0 Da), the only fragments not found being those contained in L2B (32–42) (GASKAVKQQVR^{42}). As mentioned previously, the small tripeptide and the tetrapeptide fragments deriving from tryptic digestion of this segment could easily have been lost on reversed-phase HPLC. The GASKAVK sequence is highly conserved in *B. napus* napin large chains (Fig. 5) and the GASKAVKQQVR sequence is encoded by the *B. napus* gNAP1 gene (sequence 5, Fig. 5).

L2B differs from the other five long chains in having R^{76} in place of an otherwise highly conserved P residue (Fig. 5). This was deduced from the sequence, mass and abundance of the fragment L2(3) (Table 1, Fig. 4) identified as VCNIR^{76} of L2B. The contiguous fragment L2(10) (QVSICPFQK^{85}) arising from tryptic cleavage after R^{76} and K^{85} in L2B, was also observed (Fig. 4).

Although large subunit L2C is present as a minor entity (Table 1), the complete sequence (Fig. 5) was able to be deduced from fragments encompassing the complete sequence, except for the inferred fragment L2C (32–42) (GASKAVKQQVR^{42}) as discussed above. The calculated mass of the deduced sequence of L2C (10186.72 Da) (Fig. 5) is in precise agreement with the observed mass (10186.9 ± 1.2 Da) (Table 1).

3.3. Compositions of the disulfide-linked napin complexes

The subunit compositions of the oxidized, disulfide-linked circa 14.5 kDa napin complexes were determined from ESMS of the heat- and acid-treated CM52-binding fraction from kohlrabi seeds (Table 3). Out of a total of 36 possible combinations of 6 small and 6 large subunits in 1:1 disulfide-linked complexes, only 7 napin complexes were detected, the observed masses being in good agreement with masses calculated from the deduced sequences of the small [18] and large (Fig. 5) subunits assuming that 4 disulfides are present in the oxidized complexes (Table 3). It is notable that each large subunit (except for L2B) was found to be associated with only one particular small

Table 3
Subunit composition of the *B. napus* napin complexes

Complex	Relative intensity	Subunit composition	Average molecular mass (Da)	
			observed	calculated
C1	100%	L2A+S1A-8H	14242.6±1.7	14241.42
C2	51%	L1A+S1B-8H	13935.6±1.7	13934.12
C3	33%	L2C+S1A-8H	14614.2±0.8	14612.78
C4	30%	L1B+S1A-8H	14250.0±2	14250.41
C5	18%	L2B+S2-8H	14840.6±0.9	14840.04
C6	16%	L2B+S4-8H	14921.1±1.4	14920.13
C7	8%	L1C+S2-8H	14415.6±1.9	14416.60

The average molecular masses and relative intensities of components present in the heat- and acid-treated CM52-binding fraction from kohlrabi seeds were determined by ESMS. The 95% confidence limits are presented. The average molecular masses of the deduced complexes were calculated from the deduced sequences of the small subunits [18] and of the large subunits (Table 1) assuming that 4 disulfides are present in the fully oxidized napin complexes.

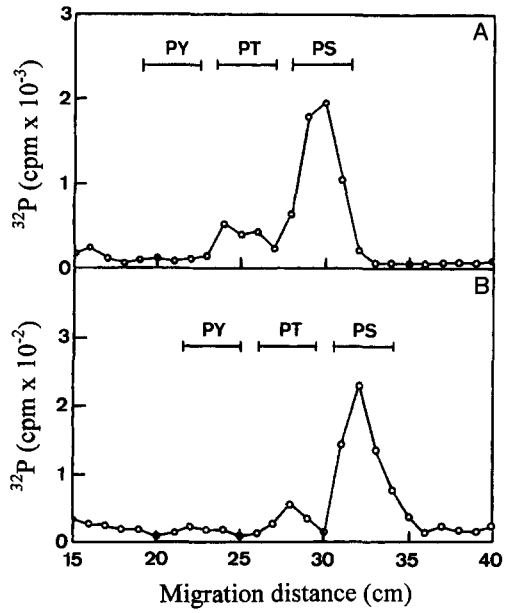

Fig. 6. Phosphoamino acid analysis of fraction L1 and L2 napin large chains phosphorylated by wheat CDPK. Phosphoamino acid analyses of acid hydrolysates of [^{32}P]phosphoL2 (A) and of [^{32}P]phosphoL1 (B) were conducted as described in Section 2. The locations of the ninhydrin-positive zones corresponding to the phosphoamino acid standards are indicated, namely phospho-L-tyrosine (PY), phospho-L-threonine (PT) and phospho-L-serine (PS).

subunit. L2B is present in similar amounts in complexes with both S2 and S4 (Table 3). However, certain small subunits (S1A and S2) were found to be associated with more than one type of large subunit (Table 3). No evidence was found for complexes involving small subunits S3A and S3B, noting that these subunits are identical to S1A and S1B, respectively, except for having an additional C-terminal W residue [18].

3.4. Phosphorylation sites of napin large subunits

The major kohlrabi seed basic CDPK substrate fraction resolved by gel filtration was phosphorylated in a reaction involving wheat CDPK and [γ-^{32}P]ATP and subsequently purified by reversed-phase HPLC, after which the radioactive labelling of large chain fraction L2 (0.01 mol/mol) was found to be much greater than that of large chain fraction L1 (0.001 mol/mol) [18]. The leading half of fraction L2 contained mainly L2B (on the basis of ESMS) and was labelled to approximately the same degree as the trailing half of fraction L2, which contained mainly L2A and a lesser quantity of L2C (Table 1). Phosphoamino acid analysis of [^{32}P]phosphoL1 and [^{32}P]phosphoL2 preparations revealed that phosphorylation in both cases occurs primarily on serine residues and to a lesser extent (approx. 20%) on threonine residues (Fig. 6). It should be noted that wheat CDPK is a serine/threonine-specific protein kinase [22].

We have previously found that phosphorylated peptides can elute just prior to the dephosphopeptide in the HPLC system employed for this study [23–26]. After HPLC of the tryptic digest of [^{32}P]phosphoL2, the major peak of radioactivity (peak 5, Fig. 2) elutes just prior to peak components L2(6) (L2A (59–68); IYQTATHLPK^{68}), L2(7)a (L2B/C (62–71); IYQTATHLPR^{71}), L2(7)b (L2A (69–88); VCNIPQVSVCPFQKTMPGPS^{88}), L2(8)a (L2A (43–58); QQQGQQGQQLQQVISR^{58}) and L2(8)b (L2B/C (43–61); QQGQQQGQQGQQLQQVISR^{61}) (Figs. 2, 4 and 5). Assuming that this major site of phosphorylation is on a serine eliminates L2A (59–68) and L2B/C (62–71) as phosphorylated sequences. There is no evidence for TMPGPS phosphorylation: L1A contains this C-terminal sequence and is very poorly phosphorylated (Figs. 1 and 5) and there is no peak of radioactivity eluting with or prior to L2(1) (L2A (83–88); TMPGPS^{88}). Accordingly the C-terminal S^{88} of fragment L2(7)b (L2A (69–88)) can be eliminated as a site of phosphorylation. S^{76} on the same fragment is eliminated as a major site of phosphorylation since other fraction L2-derived fragments containing the equivalent of L2A S^{76} (L2(11), L2(12)a, L2(12)b and L2(13)) elute much later than even the minor peak of radioactivity (peak 9) (Figs. 2 and 4). Accordingly we conclude that the peak 5 radioactivity is associated with the phosphorylated form of L2(8)a and L2(8)b (Fig. 2), the phosphorylated residues being S^{57} of L2A and S^{60} of L2B and L2C (Fig. 4) within the identical sequence LQQVI*S*RIYQTAT. We have found that a particular *Sinapis alba* napin large chain is phosphorylated on the corresponding serine within the near-identical sequence LQHVI*S*^{60}RIYQTAT (Neumann, Condron and Polya, unpublished data).

The L1 preparation is poorly phosphorylated by CDPK (0.001 mol/mol) as compared to the L2 preparation (0.01 mol/mol) [18]. Reversed-phase HPLC of a tryptic digest of a [^{32}P]phosphoL1 preparation yields a broad spread of radioactivity across the profile but with 2 elevated zones associated with peaks 12 and 13 (Fig. 1). Peak 12 corresponds to the oxidized fragments L1A (1–31) (PQG—PTLK^{31}) and L1B/C (1–31) (SQG—PTLK^{31}) (Fig. 3). The reduced forms of these fragments are expected to elute at a higher CH_3CN concentration than the oxidized forms (e.g., see Fig. 4) and indeed a second peak of radioactivity is observed eluting at about 41% CH_3CN (peak 13, Fig. 3). This could indicate a possible phosphorylation site on T^{29} within the sequence CVCP*T*LK^{31}.

3.5. Calmodulin antagonist activity of kohlrabi napin short and long chains

The fraction from kohlrabi seed extracts that binds to CM52 and is resolved on gel filtration as a low molecular weight peak of protein with CDPK substrate activity [18] inhibits calmodulin (CaM)-dependent myosin light chain kinase (MLCK) (IC_{50} value 3.8 ± 1.3 μM). A similar fraction resolved from rape seed (*B. napus*) also inhibits MLCK (IC_{50} value 3.5 ± 0.7 μM), as does the basic

fraction from turnip seed extract that binds to CM52 (IC_{50} value 1.6 ± 0.5 μM).

The napin small chain fractions from kohlrabi seeds as resolved by reversed-phase HPLC are all MLCK inhibitors [18] and so are the large chains. The IC_{50} values for the large chain fractions L1 and L2 are 3.2 ± 0.7 μM and 1.3 ± 0.6 μM, respectively. Additional confirmation of the CaM antagonist activity of the kohlrabi napins was obtained from examination of Ca^{2+}-dependent fluorescence enhancement of dansyl-CaM. 10 μM kohlrabi CM52-binding fraction largely abolishes this phenomenon [18], indicative of the presence of CaM antagonist proteins [20].

4. Discussion

The procedures described in this paper and the accompanying paper [18] permit the rapid purification of a multiplicity of napin short chains and long chains from kohlrabi seeds. Application of ESMS has enabled the identification of these individual subunits through the precise determination of their average molecular masses. The application of ESMS and Edman sequencing to tryptic fragments of these proteins has enabled the determination of the amino acid sequences of 6 copurifying small chains and 6 co-purifying large chains in agreement with the overall masses of these polypeptides. The analysis was complicated by the existence of a multiplicity of large chains. Nevertheless the complete sequence of L1A is in precise agreement with the overall mass and the masses of the tryptic fragments and is identical to the protein encoded by a *B. napus* napin gene [6] (sequence 1, Fig. 5) except for the absence of a C-terminal Y residue in L1A (Fig. 5). The complete sequences of the other large chains L2A, L2B and L2C and the near-complete sequences of L1B and L2C have also been deduced and are precisely consistent with the observed masses of the proteins and the masses and relative abundances of the tryptic fragments found. It is notable that none of the calculated masses of the published protein- or DNA-based *B. napus* large chain sequences correspond to the masses of the isolated large chains (Table 1; Fig. 5) with the exception of the des-Y^{91} *B. napus* gene product [6] which is identical to L1A (sequence 1, Fig. 5).

The finding that L1A is linked only to small subunit S1B (Table 3) is exactly in accord with the sequences of corresponding *B. napus* napin cDNAs [2,6]. S1B and L1A are encoded by the same gene and the S1B-L1A complex evidently derives from processing of a large polypeptide precursor [2,6]. It should be noted that the *B. napus* pN2 napin cDNA [1] encodes a large subunit identical to L1A but the encoded small subunit has a C-terminal N instead of the C-terminal S of S1B [1,18].

Of the 6 napin large chains resolved and sequenced only the L2 fraction napin large chains are phosphorylated well and this evidently occurs on S^{57} in L2A and on S^{60} in L2B and L2C. The phosphorylated residue occurs in the common sequence LQQVI*S*RIYQTAT. Plant CDPK phosphorylates a variety of synthetic peptides having a Basic-X-X-serine(threonine) sequence at the phosphorylation site [22]. However a variety of proteins phosphorylated by plant CDPK are phosphorylated on sites having serine-X-Basic [22,23], serine-X-X-Basic [23], Basic-X-X-serine-X-X-Basic [27] or Basic-X-X-serine-X-Basic [28] phosphorylation site sequences. The L2 fraction napin large chain phosphorylation site is the first example we have found of a serine-Basic phosphorylation site motif in a plant protein phosphorylated by plant CDPK. We have recently established the sequence of a *S.alba* napin large chain that is identical to the *S.alba* SinaI large chain [8] except for an additional LQH sequence in the *LQH*VISRIY^{63} region corresponding to the LQQVISRIY^{60} sequence of L2A and the LQQVISRIY^{63} sequence of L2B and L2C (Fig. 5). The *S.alba* napin large chain is phosphorylated on S^{60} in this sequence (Neumann and Polya, unpublished data). There is no evidence for phosphorylation of the corresponding serine residues S^{55}, S^{57} and S^{57} in the *B. napus* napin L1 fraction large chains L1A, L1B and L1C, respectively (Fig. 5). It is not clear what features of the L1 fraction *B. napus* large chain sequences in this region (Fig. 5) hinder such phosphorylation. As discussed in the accompanying paper [18], the low phosphorylation stoichiometry observed does not preclude a physiological function. The function (if any) of the large chain phosphorylation is not known.

We have previously shown that *R.sativus* napin small chains are calmodulin (CaM) antagonists, inhibiting CaM-dependent MLCK [15]. The CaM antagonist activity of *R.sativus* seeds (as measured through inhibition of CaM-dependent cyclic nucleotide phosphodiesterase) disappear (together with napin-size polypeptides) during seed germination [17]. The present study shows that large napin chains as well as napin small chains are CaM antagonists and it is therefore useful to consider common structural features of these two napin subunits. The napin small chains of the Brassicaceae have a central 23 amino acid, Q-rich and basic amino acid-containing region bounded by relatively short N-terminal and C-terminal side sequences that are P-, A/G- and P-, A/G- and S-containing, respectively. For each napin small chain amphipathic helix wheel projection analysis [29,30] shows that the central region has the potential to form an α-helix in which all the basic residues are located on one side [15,18]. A variety of proteins that interact with CaM have CaM-interacting domains that form amphipathic α-helices, including helices in which all the basic residues are located on one side of the helix [29,30]. Application of this analysis to the kohlrabi napin small chain sequence R^{11}-Q^{30} (common to all 6 small chains resolved in this study) reveals that all the basic (R,K,H) residues are confined to a 220° sector of the projection circle [15,18]. As discussed previously, it is likely that this sequence element with a propensity to form

1.	Small chains	R^{11} K E F Q Q A Q H L R A C Q Q W L H K Q A M Q^{33}	(S1A)	[220°]
2.	Large chains	L^{10} L Q Q C C N E L H Q^{20}	(L1A)	[180°]
3.	L1A	L^{30} K G A S K A V K Q Q I Q Q Q G Q Q Q^{48}		[160°]
	L2A	L^{30} K G A S K A V K Q Q V R Q Q Q G Q Q^{48}		[160°]
	L2B, L2C	L^{30} K G A S K A V K Q Q V R Q Q G Q Q Q^{48}		[160°]
4.	L1A	Q^{51} Q M V S R I Y Q T A T H L^{64}		[200°]
	L1B, L1C	Q^{53} Q I V S R I Y Q T A K H L^{66}	(L1B)	[200°]
	L2A, L2B, L2C	Q^{51} L Q Q V I S R I Y Q T A T H L^{66}	(L2A)	[200°]

Fig. 7. Amphipathic α-helical wheel projection analysis applied to *B. napus* small and large chain sequences. One small chain sequence region [18] and three large chain sequence regions are considered. Where the amino acid numbering differs for different chains the numbering for one (indicated in parentheses) is given. The results of the wheel projection analysis are presented in a linear fashion with 'basic side' residues underlined (1 and 3) or 'polar side' residues underlined (2 and 4). The sector of the α-helix projection wheel to which all of the underlined residues are confined is given in degrees in square brackets in each case.

a '2-sided' helix is involved in the CaM antagonist activity of the *B. napus* small chains [15,18].

The *B. napus* napin large chains are also CaM antagonists and indeed the small and large chains have regions with similar structures. It has been pointed out previously that *S.alba* napin small and large chains have similar N-terminal sequences and similar C-terminal sequences [12]. The *B. napus* napin small and large chains also have similar P-, A/G- and R-containing N-terminal 9 to 11 amino acid sequences [18] (Fig. 5) and have similar P-, A/G- and Q- and hydrophobic amino acid-containing C-terminal 10 to 16 amino acid sequences [18] (Fig. 5). However inspection of other regions of the napin large chains for potential α-helix-forming sequences reveals 3 such regions.

The L^{10}LQQCCNELHQ^{20} sequence of L2B that is common to all 6 *B. napus* long chains sequenced here and is bracketed between proline residues PP^{9} and P^{23} (Fig. 5) can potentially form an α-helix in which all but one of the polar residues are located on one side and all of the hydrophobic residues (including oxidized cysteines) are confined to the other half (group 2, Fig. 7).

The region of the *B. napus* napin large chains that is most similar to the central putative helical region of the small chains is the central sequence (corresponding to L^{30}-Q^{48} of L1A) that is rich in Q and basic residues (Fig. 5). This region is bracketed between a conserved proline (P^{28} in L1A) and a variable 2 to 7 amino acid Q-, S-, G- and K-containing region (GK^{50} in L1A) (Fig. 5). Application of amphipathic helix wheel projection analysis to this central sequence of the completely sequenced large chains shows that it has the potential to form a '2-sided' α-helix (group 3, Fig. 7). This is similar to those predicted for the corresponding napin small chain sequence (group 1, Fig. 7) in that, Q residues apart, all other polar residues (and notably K and R residues) are confined to one side of the putative α-helix. The remaining part of the projection circle contains Q and nonpolar residues (group 3, Fig. 7).

A third element that could be involved in interactions with CaM (or indeed with membranes) is a putative amphipathic α-helix that is defined by a relatively conserved sequence present in all 6 *B. napus* napin large chains and located between the variable central region (terminating in K^{50} in L1A) and a conserved proline (P^{65} in L1A) (Fig. 5). This sequence in the L1 fraction and L2 fraction napin large chains can potentially form amphipathic α-helices in which all polar residues are confined to a 200° sector of the projection circle (group 4, Fig. 7). An amphipathic α-helix of this third kind predicted to occur in the *B. napus* napin large chain (group 4, Fig. 7) occurs in the peptide melittin, a protein that can also form a pore structure in membranes [31]. It is notable that the major phosphorylation site of the L2 fraction napin large chains occurs on the serine (S^{57} in L2A) located in the middle of this sequence element. Such phosphorylation would change the net charge and polarity of this amphipathic element. Napin large as well as small subunits [15,18] are CaM antagonists and we surmise that the common central basic residue- and Q-rich putative '2 sided α-helix' structure is involved in this interaction. Napins, in addition to being protease inhibitors, have antifungal properties [4,14] and can act synergistically with α- and β-thionins as antifungal proteins [14]. It is possible that the presumed amphipathic α-helices of the napin large chains could be involved in membrane or membrane protein interactions contributing to the antifungal action of these proteins.

Acknowledgements

This work was supported by a grant to G.M.P. from the Australian Research Council. We are grateful to D.R.

Bannon for computer programs used in calculating average molecular masses from amino acid sequences.

References

[1] Crouch, M.L., Tenbarge, K.M., Simon, A.E. and Ferl, R. (1983) J. Mol. Appl. Genet. 2, 273–283.

[2] Josefsson, L-G., Lenman, M., Erickson, M.I. and Rask, L. (1987) J. Biol. Chem. 262, 12196–12201.

[3] Krebbers, E., Herdies, L., De Clerco, A., Seurinck, J., Leemans, J., Van Dammes, J., Segura, M., Gheysen, G., Van Montagu, M. and Vandekerckhove, J. (1988) Plant Physiol. 87, 859–866.

[4] Terras, F.R.G., Schoofs, H.M.E., De Bolle, M.F.C., Van Leuven, F., Rees, S.B., Vanderleyden, J., Cammue, B.P.A. and Broekaert, W.F. (1992) J. Biol. Chem. 267, 15301–15309.

[5] Bruix, M., Jiménez, M.A., Santoro, J., González, C., Colilla, F.J., Méndez, E. and Rico, M. (1993) Biochemistry 32, 715–724.

[6] Ericson, M.L., Rödin, J., Lenman, M., Glimelius, K., Josefsson, L-G. and Rask, L. (1986) J. Biol. Chem. 261, 14576–14581.

[7] Scofield, S.R. and Crouch, M.L. (1987) J. Biol. Chem. 262, 12202–12207.

[8] Menéndez-Arias, L., Moneo, I., Domínguez, J. and Rodríguez, R. (1988) Eur. J. Biochem. 177, 159–166.

[9] Svendsen, I.B., Nicolova, D., Goshev, I. and Genov, N. (1989) Carlsberg Res. Commun. 54, 231–239.

[10] Baszczynski, C.L. and Fallis, L. (1990) Plant Mol. Biol. 14, 633–635.

[11] Raynal, M., Depigny, D., Grellet, F. and Delseny, M. (1991) Gene 99, 77–86.

[12] Ericson, L., Murén, E., Gustavsson, H.-O., Josefasson, L-G. and Rask, L. (1991) Eur. J. Biochem. 197, 741–746.

[13] González, de la Rena, M.A., Villalba, M., Garcia-López, J.L., and Rodríguez, R. (1993) Biochem. Biophys. Res. Commun. 190, 648–653.

[14] Terras, F.R.G., Schoofs, H.M.E., Thevissen, K., Osborn, R.W., Vanderleyden, J., Cammue, B.P.A. and Broekaert, W.F. (1993) Plant Physiol. 103, 1311–1319.

[15] Polya, G.M., Chandra, S. and Condron, R. (1993) Plant Physiol. 101, 545–551.

[16] Svendsen, I.B., Nicolova, D., Goshev, I. and Genov, N. (1994) Int. J. Peptide Protein Res. 43, 425–530.

[17] Cocucci, M. and Negrini, N. (1988) Plant Physiol. 88, 910–914.

[18] Neumann, G.M., Condron, R., Thomas, I. and Polya, G.M. (1996) Biochim. Biophys. Acta 1295, 23–33.

[19] Lucantoni, A. and Polya, G.M. (1987) FEBS Lett. 221, 33–36.

[20] Jinsart, W., Ternai, B. and Polya, G.M. (1991) Plant Sci. 78, 165–175.

[21] Hunkerpiller, M.W. (1985) Applied Biosystems Protein Sequence User Bulletin No. 14, Nov. 18.

[22] Polya, G.M., Morrice, N.A. and Wettenhall, R.E.H. (1989) FEBS Lett. 253, 137–140.

[23] Neumann, G.M., Condron, R. and Polya, G.M. (1994) Plant Sci. 96, 69–79.

[24] Neumann, G.M., Condron, R., Svensson, B. and Polya, G.M. (1993) Plant Sci. 92, 159–167.

[25] Neumann, G.M., Condron, R., Thomas, I. and Polya, G.M. (1994) Biochim. Biophys. Acta 1209, 183–190.

[26] Neumann, G.M., Condron, R., Thomas, I. and Polya, G.M. (1995) Plant Sci. 107, 129–145.

[27] Weaver, C.D. and Roberts, D.M. (1992) Biochemistry 31, 8954–8959.

[28] Chang, A., Condron, R., Neumann, G.M. and Polya, G.M. (1995) Biochim. Biophys. Acta 1244, 317–324.

[29] O'Neil, K.T. and De Grado, W.F. (1990) Trends Biochem. Sci. 15, 59–64.

[30] James, P., Vorherr, T. and Carafoli, E. (1995) Trends Biochem. Sci. 20, 38–42.

[31] Vogel, H. and Jähnig, F. (1986) Biophys. J. 50, 573–582.